J. Appl. Glycosci., **71**, 55−62 (2024)
doi:10.5458/jag.jag.JAG-2023_0017

Regular Paper

Thermotolerance Mechanism of Fungal GH6 Cellobiohydrolase. Part I. Characterization of Thermotolerant Mutant from the Basidiomycete *Phanerochaete chrysosporium*

(Received December 18, 2023; Accepted March 14, 2024)

Sora Yamaguchi,[1] Naoki Sunagawa,[1] Masahiro Samejima,[1,*] and Kiyohiko Igarashi[1,†]

[1] *Department of Biomaterial Sciences, Graduate School of Agricultural and Life Sciences, The University of Tokyo* (*1−1−1 Yayoi, Bunkyo-ku, Tokyo 113−8657, Japan*)

Abstract: Cellobiohydrolase (CBH), belonging to glycoside hydrolase family 6 (GH6), plays an essential role in cellulose saccharification, but its low thermotolerance presents a challenge in improving the reaction efficiency. Based on a report that chimeric CBH II (GH6) engineered to remove non-disulfide-bonded free Cys shows increased thermotolerance, we previously mutated the two free Cys residues to Ser in GH6 CBH from the basidiomycete *Phanerochaete chrysosporium* (*Pc*Cel6A) and obtained a thermotolerant double mutant, C240S/C393S (Yamaguchi *et al*., J. Appl. Glycosci. 2020; 67: 79−86). Here, characterization of the double mutant revealed that its activity towards both amorphous and crystalline cellulose was higher than that of the wild-type enzyme at elevated temperature, suggesting that the catalytic domain is the major contributor to the increased thermotolerance. To investigate the role of each free Cys residue, we prepared both single mutants, C240S and C393S, of the catalytic domain of *Pc*Cel6A and examined their residual activity at high temperature and the temperature-dependent changes of folding by means of circular dichroism measurements and thermal shift assay. The results indicate that the C393S mutation is the main contributor to both the increased thermotolerance of C240S/C393S and the increased activity of the catalytic domain at high temperature.

Key words: cellulose, cellobiohydrolase, GH6, thermotolerance, free cysteine, circular dichroism

INTRODUCTION

Lignocellulose is the most abundant carbon stock in nature, and furthermore is a renewable resource with the potential to replace fossil resources as a raw material for biofuels and bioproducts. In particular, enzymatic saccharification of lignocellulose does not require strong acids, bases, or heat and is expected to be a less energy-consuming conversion method than chemical or physical processing. One of the main components of lignocellulose is cellulose, which can be hydrolyzed by cellulase from microorganisms such as fungi and bacteria. Cellulases acting on cellulose polymer are mainly classified into cellobiohydrolase (CBH), which can hydrolyze crystalline cellulose from the end of the chain, and endoglucanase, which randomly hydrolyzes the chains of amorphous cellulose. Since crystalline cellulose is not easily hydrolyzed due to its tightly packed structure, CBH is considered a key cellulase for the efficient enzymatic saccharification of cellulose.

Fungal CBH is classified as glycoside hydrolase family 6 (GH6, EC 3.2.1.91) or 7 (GH7, EC 3.2.1.176) in the Carbohydrate-Active enZymes database [1]. Most of the GH6 CBH and GH7 CBH family members have a carbohydrate-binding module (CBM) connected to the catalytic domain via a flexible linker [2, 3], and the two families act synergistically [4−6], with GH6 CBH working from the non-reducing end and GH7 CBH from the other end [7]. For industrial-scale enzymatic saccharification, high temperatures are preferred in order to increase the hydrolysis rate. However, the thermotolerance of GH6 CBHs is generally lower than that of GH7 CBHs [8, 9], and thus the loss of synergistic effects is an issue. To address this, various attempts have been made to enhance the stability of GH6 CBH at higher temperatures, including directed evolution using random mutagenesis [10], recombination of sequence blocks from different GH6 CBHs [11], consensus mutagenesis and accumulation of advantageous mutations [12].

A notable recent finding from Arnold's lab was that mutation of free (non-disulfide-forming) Cys residues in an engineered chimeric GH6 CBH was effective for improving thermotolerance [13, 14]. Building on that work, we previously mutated the two free Cys residues of GH6 CBH from the basidiomycete *Phanerochaete chrysosporium* (*Pc*Cel6A) [15], obtaining a double mutant that exhibited higher activity than the wild-type (WT) enzyme at elevated temperature. However, we did not establish how each free Cys substitution affected the activity and folding of the enzyme at high temperatures.

In this study, therefore, we examined the activity and

†Corresponding author (Tel. +81−3−5841−5255, E-mail: aquarius@mail.ecc.u-tokyo.ac.jp, ORCID ID: 0000-0001-5152-7177)
*Present address: Faculty of Engineering, Shinshu University (4−17−1 Wakasato, Nagano 380−8553, Japan).

Abbreviations: CBH, cellobiohydrolase; CBM, carbohydrate-binding module; CD, circular dichroism; GH6, glycoside hydrolase family 6; GH7 glycoside hydrolase family 7; PASC, phosphoric-acid-swollen cellulose; T_m, melting temperature; WT, wild type

folding of *Pc*Cel6A mutants with free Cys substitution(s) in order to characterize the role of each free Cys residue in determining the thermotolerance of GH6 CBH.

MATERIALS AND METHODS

Materials. DNA polymerase PrimeSTAR Max (Takara Bio Inc., Shiga, Japan) was used to amplify the DNA of *Pc*Cel6A single mutants (C240S and C393S). Yeast extract (BD Biosciences, Franklin Lakes, NJ, USA), peptone (Nihon Pharmaceutical Co., Ltd, Tokyo, Japan), and glycerol (FUJIFILM Wako Pure Chemical Corporation, Osaka, Japan) were used to prepare the culture medium. *Pichia pastoris* strain KM71H (Thermo Fisher Scientific Inc., Waltham, MA, USA) was used for heterologous expression of the mutant enzyme. D-Glucose (FUJIFILM Wako Pure Chemical Corporation), cellobiose (Sigma-Aldrich, St. Louis, MO, USA), and cellotriose (Megazyme Ltd., Bray, Ireland) were used as standards for activity measurement.

Expression. The pPICZα vector encoding full-length *Pc*Cel6A WT and C240S/C393S was constructed, and *P. pastoris* was transformed in a previous study of WT [16] and C240S/C393S[15] respectively. Colonies were grown for about 24 h in 5 mL of 1 % (w/v) yeast extract, 2 % (w/v) peptone medium, supplemented with 2 % (w/v) glycerol (YPG) medium at 30 ˚C. The culture was added to 200 mL of YPG medium and grown for about 24 h at 30 ˚C. Expression was induced in 40 mL of 1 % (w/v) yeast extract, 2 % (w/v) peptone (YP) medium at 26.5 ˚C by adding methanol to give a final concentration of 1 % (v/v) every other day. The third-day culture was centrifuged at 3,000 × G for 10 min, and the supernatant was centrifuged again at 15,000 × G for 10 min, at 4 ˚C.

The pPICZα vector encoding the catalytic domain of *Pc*Cel6A WT was prepared in a previous study [17], and that of *Pc*Cel6A C240S/C393S was prepared by deleting the CBM-linker region (residues 1−81) as previously described [15]. The pPICZα vectors encoding single mutations in the catalytic domain of *Pc*Cel6A were constructed by inverse PCR using the primers listed in Table S1 (see J. Appl. Glycosci. Web site), and *P. pastoris* was transformed as previously described [15]. Colonies were grown in 200 mL of YPG medium and expression was induced as mentioned above. The fifth-day culture was centrifuged as above and the supernatant was filtered with a syringe filter (Millex-GV Syringe Filter Unit, 0.22 μm, PVDF, 33 mm, gamma sterilized, Merck KGaA). The molecular weight of the proteins was estimated by SDS-PAGE using 12 % polyacrylamide gel.

Purification. Full-length *Pc*Cel6A C240S/C393S was purified as follows. Ammonium sulfate was added to the enzyme solution to give the final concentration of 1 M, and the mixture was applied to a 175 mL TOYOPEARL Phenyl-650M column (Tosoh Corporation, Tokyo, Japan) equilibrated with the same molarity of ammonium sulfate in 20 mM sodium acetate buffer (pH 5.0). The enzyme was eluted with an 875 mL linear gradient from the same molarity to 0 M ammonium sulfate in the same buffer. The enzyme fractions were concentrated, and its buffer was exchanged with 20 mM Tris-HCl buffer (pH 8.0) using the ultrafiltration disc (5 kDa NMW; Merck KGaA). The eluate was applied to a 150 mL TOYOPEARL DEAE-650 column (Tosoh Corporation) equilibrated with the same buffer and eluted with a 1,500 mL linear gradient from 0 to 0.5 M NaCl in the same buffer. The molecular weight of the protein was estimated by SDS-PAGE using 12 % polyacrylamide gel. The fractions with a few kilodaltons lower molecular mass devoid of *N*-glycosylation were collected.

The catalytic domain of *Pc*Cel6A was purified as follows. Ammonium sulfate and sodium acetate buffer (pH 5.0) were added to the enzyme solution to give final concentrations of 1 M and 20 mM, respectively. The solution was applied to a 5 mL TOYOPEARL Phenyl-650M column (Tosoh Corporation) equilibrated with the same molarity of ammonium sulfate in 20 mM sodium acetate buffer (pH 5.0) and eluted with a 25 mL linear gradient from the same molarity to 0 M ammonium sulfate in the same buffer. The enzyme fractions were concentrated, and its buffer was exchanged with 20 mM Tris-HCl buffer (pH 8.0) using a Vivaspin™ 20-5K (Sartorius, Göttingen, Germany). The solution was applied to a 16 mL TOYOPEARL DEAE-650 column (Tosoh Corporation) equilibrated with 20 mM Tris-HCl buffer (pH 8.0). The enzyme was eluted with an 80 mL linear gradient from 0 to 50 mM NaCl in the same buffer. The fractions were concentrated with a Vivaspin™ 20-5K (Sartorius), and its buffer was exchanged with 20 mM Tris-HCl buffer (pH 8.0) containing 20 mM NaCl using a PD-10 desalting column packed with Sephadex G-25 resin (Cytiva). The solution was concentrated with a Vivaspin™ 500-5K (Sartorius) or diluted to 20 μM.

Activity measurements of full-length enzyme. Activity measurements of full-length *Pc*Cel6A C240S/C393S were conducted in a 2.0 mL Protein LoBind Tube (Eppendorf Corporate, Humburg, Germany) with a total volume of 1,800 μL. The activity of *Pc*Cel6A WT purified previously [16] was also measured for comparison. One micromolar *Pc*Cel6A was incubated with 0.25 % (w/v) PASC [18] or 0.05 % (w/v) cellulose III$_H$ [19] in 100 mM sodium acetate buffer (pH 5.0) at 30, 45, or 60 ˚C for 6 h with rotation in a thermo block rotator (Nissinrika, Tokyo, Japan). The pH was chosen based on a previous study of *Pc*Cel6A WT [20]. After 0.5, 1, 2, 3, 4, 5, and 6 h, 200 μL of solution was collected and filtered using 96-well plates with a 0.22 μm filter (MultiScreen® Filter Plates, Merck KGaA). The filtrate was diluted with acetonitrile and distilled water. The diluted solution was kept overnight at 4 ˚C and filtered the following day. The cellobiose concentration in the filtrate was determined by HPLC with a Corona™ Charged Aerosol Detector™ (ESA Biosciences Inc., Chelmsford, MA, USA) as previously described [16].

Activity measurements of the catalytic domain. Activity measurements of the catalytic domain of *Pc*Cel6A were conducted using a 96-well plate with a volume of 150 μL per well at 30, 45, or 60 ˚C with shaking at 1,000 rpm in an incubator (Deep Well Maximizer Micro BioShaker M-BR-022UP, Taitec Corporation, Saitama, Japan). The reaction solution comprised 0.5 μM *Pc*Cel6A, 0.25 % (w/v) PASC, and 20 mM sodium acetate buffer (pH 5.0). The solution was filtered after 4 h using 96-well plates with a 0.22 μm filter (MultiScreen® Filter Plates, Merck KGaA) and diluted with an equal volume of acetonitrile. As described above, the dilute solution was kept overnight at 4 ˚C and filtered again the following day.

The filtrate was separated on a Shodex HILICpak VG-50 4E (Resonac Holdings Corporation, Tokyo, Japan) with acetonitrile/H_2O = 75/25 v/v. Products were quantified as described above using glucose, cellobiose, and cellotriose as standards.

Circular dichroism measurements. Circular dichroism at 214 nm was measured on a spectropolarimeter (J-820; JASCO Corporation, Tokyo, Japan) equipped with a Peltier cell holder (PTC-423L; JASCO Corporation) using a 5 mm path length quartz cell (JASCO Corporation), Teflon stirring bar (JASCO Corporation), and silicon cap (JASCO Corporation). The temperature gradient was 1 ˚C/min, and data was acquired every 5 ˚C. The enzyme concentration was 0.8 μM in 2 mM sodium acetate (pH 5.0), 0.2 mM Tris-HCl (pH 8.0), and 0.2 mM NaCl. The melting temperature (T_m) was defined as the midpoint of the sigmoidal curve regressed to the negative-peak plots of molar ellipticity at 214 nm.

Thermal shift assay. Thermal shift assay was carried out in a total volume of 20 μL in a 96-well PCR tube using a Mx3000P Real-Time QPCR System (Agilent Technologies, Inc., Santa Clara, CA, USA) and SYPRO™ Orange Protein Gel Stain (5,000x Concentrate in DMSO; Thermo Fisher Scientific Inc.). The buffer was sodium phosphate at pH 3, 6, 7, and 8 and sodium acetate at pH 4 and 5. With the plate on ice, 0.1 mg/mL protein was mixed with 50 mM buffer and 5x SYPRO™ Orange in each well, and the plate was sealed and spun down with a vegetable drainer (Yamaken Kogyo, Niigata, Japan). The temperature was ramped up in 0.5 ˚C/min increments from 25 to 95 ˚C. The excitation and emission wavelengths were 490 and 580 nm, respectively. The T_m under each condition was calculated as the midpoint of the dissociation curve between the lowest and highest fluorescence intensity. Amino acid hydrophobicity was visualized with the PyMOL Molecular Graphics System (v.2.4.2; Schrödinger, LLC) according to the normalized consensus hydrophobicity scale [21].

RESULTS AND DISCUSSION

Time course of activity of the thermotolerant double mutant at different temperatures.

*Pc*Cel6A has six Cys residues in the catalytic domain, four of which form disulfide bonds, C171−C230 and C361−C408, while the remaining two, C240 and C393, are free (Fig. 1). C240 is located in the α-helix relatively close to the enzyme surface, and C393 is on the C-terminal loop (residues 390−425) that encloses the substrate together with the N-terminal loop (residues 172−177). The time courses of hydrolytic product formation from PASC and cellulose IIII by WT and C240S/C393S were different, depending on the incubation temperature. When incubated with PASC at 30 and 45 ˚C, the time course of C240S/C393S was almost the same as that of WT (Figs. 2A and 2B), but the activity of C240S/C393S towards PASC was higher than that of WT at 60 ˚C (Fig. 2C). A similar tendency was seen when cellulose IIII was used as a substrate (Figs. 2D, 2E, and 2F). The observation that C240S/C393S produced more product than WT from both amorphous and crystalline cellulose indicates that the thermotolerance of C240S/C393S stems from the catalytic domain rather than the CBM.

Activity of single mutants of the catalytic domain at different temperatures.

To focus on the effects of free Cys, CBM and the linker region were removed, and single mutants of the catalytic domain were prepared. As shown in Fig. 3, the main hydrolysis product generated by the catalytic domain of *Pc*Cel6A was cellobiose, followed by glucose and cellotriose. Compared to the reaction at 30 ˚C, a large amount of cellobiose was produced by WT and all three mutants at 45 ˚C. In contrast, there was no significant difference in the cellobiose concentrations produced by WT at 60 ˚C, compared to 45 ˚C. However, the amount of cellobiose produced by C240S was significantly lower at 60 ˚C than at 45 ˚C, while the amounts produced by C393S and C240S/C393S were significantly higher at 60 ˚C than at 45 ˚C. There was no significant difference between C393S and C240S/C393S.

As discussed in our previous study, the activity at a higher reaction temperature could reflect the increase in the activity due to the larger kinetic energy in competition with the decrease in the activity due to the thermal inactivation of the enzyme. The reason why the activity did not significantly increase at 60 ˚C compared to 45 ˚C in the present study would mean that the effect of larger kinetic energy and the enzyme's thermal inactivation were roughly equivalent. In the previous study from Arnold's lab, free Cys of thermotolerant chimeric GH6 CBH, corresponding to C240 of *Pc*Cel6A, was substituted with Ala, Gly, Lys, and Ser [14]. The residual activity of the mutants towards microcrystal-

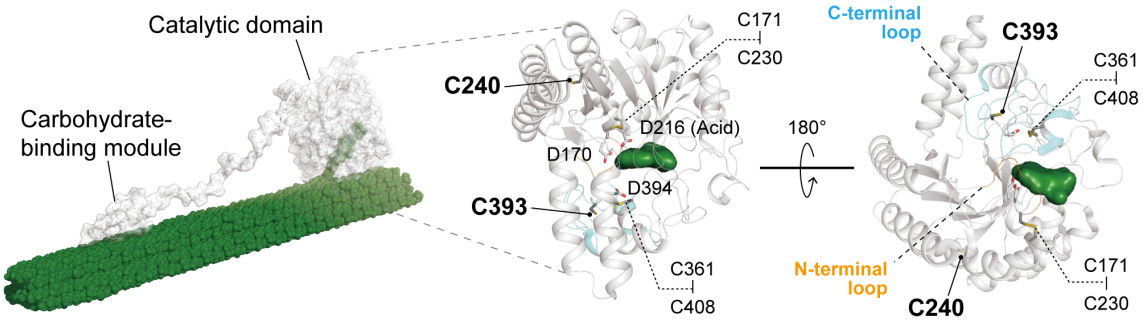

Fig. 1. Location of cysteine residues in *Pc*Cel6A.

The overall structure of *Pc*Cel6A (left) was created by superposing the X-ray crystal structure of the catalytic domain (PDB ID 5XCY) [17], and the carbohydrate-binding module predicted using Phyre2 [40] on the overall structure of *Tr*Cel6A modeled previously [41]. The structure of the catalytic domain (middle and right) was adopted from the X-ray crystal structure of *Pc*Cel6A in the complex with cellobiose (PDB ID 5XCZ) [17]. The side chain acid catalyst D216, candidate base catalysts D170 and D394, and Cys are shown as sticks. Cellulose and cellobiose are colored green in the overall structure and the structure of the catalytic domain, respectively.

line cellulose after thermal inactivation became much higher. Among them, the Ser mutant showed lower residual activity than the Gly or Ala mutant. These results suggest that mutation with Ser at this site might result in reduced stability, compared with the introduction of smaller, non-polar residues. This is consistent with the fact that *Pc*Cel6A C240S showed lower activity at 60 ˚C than at 45 ˚C in our study. Further, our finding of increased activity of C393S is in agreement with the previous report that the 50 %-inactivation temperature was increased by 10 ˚C by mutation of the free Cys residue corresponding to C393 of *Pc*Cel6A [13].

Comparing the result from the activity measurement of the full-length enzyme (Fig. 2) and the catalytic domain (Fig. 3), the pattern of change in cellobiose production with increasing temperature appeared different at first glance. For example, in the case of WT, cellobiose production dropped considerably from 45 to 60 ˚C in Fig. 2, while it was similar in Fig. 3. This would be because the result in Fig. 3 is from the early stage of the reaction. Since the initial reaction volume and the enzyme concentration in Fig. 3 were one-twelfth and one-half of those in Fig. 2, the reaction rate in Fig. 3 could be slower than Fig. 2. Focusing on the reaction time of 30 min in Fig. 2, the concentration of cellobiose produced by WT increased from 30 to 45 ˚C, and it remained almost unchanged from 45 to 60 ˚C while that produced by C240S/C393S increased both from 30 to 45 ˚C and from 45 to 60 ˚C, as in Fig. 3. Therefore, the cellobiose yield at 4 h in Fig. 3 would be equivalent to the one at around 30 min in Fig. 2.

Evaluation of melting temperature by circular dichroism measurement and thermal shift assay.

To investigate the loss of three-dimensional structure on heating (i.e., thermal denaturation), the change in the protein folding was measured in two ways.

The first was CD measurement at 214 nm, which is due to the β-structure in the protein core [22]. β-Strands occupy about 11 % of the *Pc*Cel6A structure (PDB ID 5XCY) [17] as estimated by the Define Secondary Structure of Proteins algorithm [23], the Beta Structure Selection method [24,

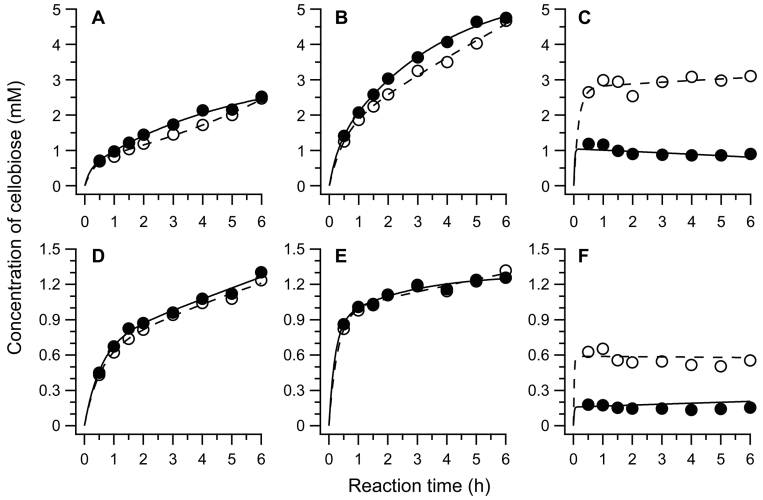

Fig. 2. Time course of cellobiose formation by full-length *Pc*Cel6A WT and C240S/C393S on PASC (A–C) and cellulose IIII (D–F).

Each enzyme (1 μM) was incubated at 30 ˚C (A, D), 45 ˚C (B, E), or 60 ˚C (C, F) with 0.25 % (w/v) PASC or 0.05 % (w/v) cellulose IIII at pH 5.0 for up to 6 h. The results for WT and C240S/C393S are shown as filled and open circles, and the fitted curves are shown as straight and broken lines, respectively.

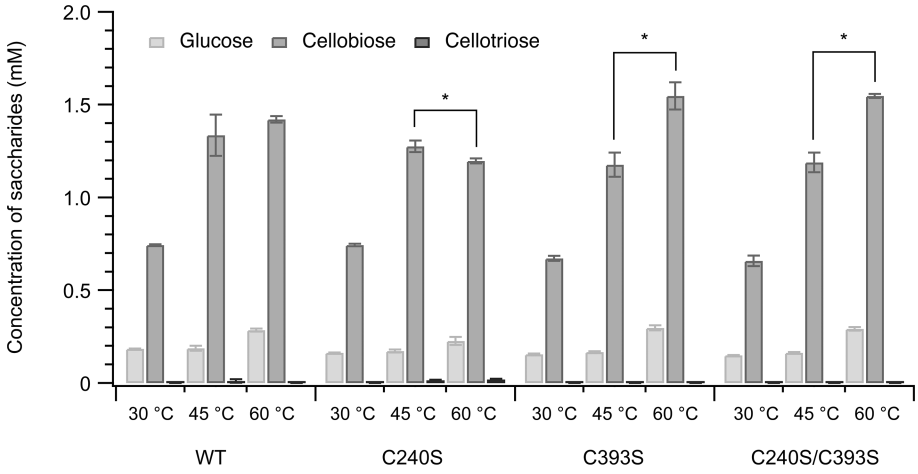

Fig. 3. Hydrolytic activity of the *Pc*Cel6A catalytic domain.

WT, C240S, C393S, or C240S/C393S (0.5 μM) was incubated at 30, 45, or 60˚C with 0.25 % (w/v) PASC at pH 5.0 for 4 h. $N = 3$, unpaired t-test, $p < 0.05$. Error bars represent ±1 standard deviation.

25], and the self-consistent method [26, 27]. The β-sheet, comprised of β-strands, is closed to form a β-barrel in the center of GH6 (Fig. 4A) [28, 29]. The temperature in the midpoint of the sigmoidal curve regressed to the negative-peak plots of molar ellipticity was considered to be T_m in the CD measurement. As can be seen from the plots and the regression curve in Fig. 4B, WT and the mutants showed a decrease of the negative peak of molar ellipticity at 214 nm as the temperature was increased from 30 to 80 ˚C, reflecting thermal denaturation of the β-structure. The measured points were fitted to a sigmoidal curve. The curves of all the mutants were shifted to the high-temperature side compared to that of WT. The T_m value of C240S/C393S (69.8 ± 1.0 ˚C) was the highest, followed by C393S (65.8 ± 0.5 ˚C), C240S (62.8 ± 0.6 ˚C), and WT (59.8 ± 0.6 ˚C) in that order. A higher T_m implies that the β-structure of the protein core is less susceptible to thermal denaturation.

The second was thermal shift assay using SYPRO Orange dye, which binds to hydrophobic regions that are usually buried inside the protein but are exposed to the outside by thermal denaturation [30]. The midpoint of the thermal denaturation curve can be taken as T_m, where half the protein is considered to remain folded, and the other half is not. The hydrophobic amino acids, to which SYPRO Orange dye binds, are located on helices pointing towards the interior and on β-structure (Fig. 5A). In the thermal shift assay at pH 3−8, the T_m values of WT, C240S, C393S, and C240S/C393S at pH 4−5 were 57−58, 59−61, 65−68, and 66−71˚C, respectively (Fig. 5B). This is consistent with the result of CD measurement, as expected, since thermal denaturation of β-structure at the protein core should lead to the exposure of the hydrophobic residues to the outside. It should be noted that pH 4−5 corresponds to the theoretical isoelectric point of *Pc*Cel6A, so the results are consistent with the idea that a greater net charge promotes unfolding due to the repulsion between charged residues [31].

The effect of mutation at C240 and C393 differed according to the reaction pH. Comparing WT *vs*. C240S (Fig. 5C) and C393S *vs*. C240S/C393S (Fig. 5D), T_m values of C240S and C240S/C393S were higher only under pH 6. On the other hand, when WT *vs*. C393S (Fig. 5E) and C240S *vs*. C240S/C393S (Fig. 5F) were compared, C393S and C240S/C393S showed higher T_m values at all pH examined. These results indicate that replacing C240 with Ser constrained thermal denaturation at under pH 6, while replacing C393 with Ser suppressed the denaturation in all pH values examined, including pH 7 and 8. A similar pH threshold was seen in the previous work on chimeric GH6 CBH. While the residual activity of normal chimeric GH6 CBH decreased sigmoidally as the temperature was increased, the mutant with a substitution of free Cys corresponding to C240 in *Pc*Cel6A showed a linear decrease of the residual activity with increasing temperature at pH 7, 8, and 9 [14]. Although the reason for this is unclear, denaturation mechanisms documented in other proteins, such as *β*-elimination of a disulfide bond [32], deamidation of the side chain of Asn and Gln [33], and succinimide formation of Glu and Asp [34], might play a role in influencing the 240th amino acid.

In addition to these potential reasons, C240 might destroy a carboxyl-carboxylate hydrogen bond. It is known that two carboxylic acids in proteins such as Asp and Glu form a strong hydrogen bond by sharing a proton between a protonated carboxyl and a deprotonated carboxylate at an intermediate pH around pH 3−6 [35]. On the other hand, the strength of the hydrogen bond becomes normal at lower pH, where both carboxylic acids are protonated, and the repulsion of the side chains occurs at higher pH, where both carboxylic acids are negatively charged. Since C240 is located relatively close to the enzyme surface and three out of four carboxylic acid pairs in the catalytic domain of *Pc*Cel6A (E101−E392, D165−E179, and D359−D412) are also exposed to outside of the enzyme, a reactive thiol of C240 and a carboxylic acid of the pair might react intermolecularly at high temperatures with high kinetic energy of molecules. Thus, it would be possible that substituting C240 enabled the strong carboxyl-carboxylate pair to be kept and led to higher T_m at pH 3−6 (Figs. 5C and 5D).

Effects of free Cys substitution on thermal denaturation.

Although C240S and C393S each have one free Cys, C393S showed a higher T_m value than C240S in CD measurement (Fig. 4B) and thermal shift assay (Fig. 5B). This might be due to the proximity of the free Cys to another Cys forming a disulfide bond, because the distance from C240 to C171, forming the nearest disulfide bond, was about 12 Å in the previously solved structure of *Pc*Cel6A WT (PDB ID 5XCY)

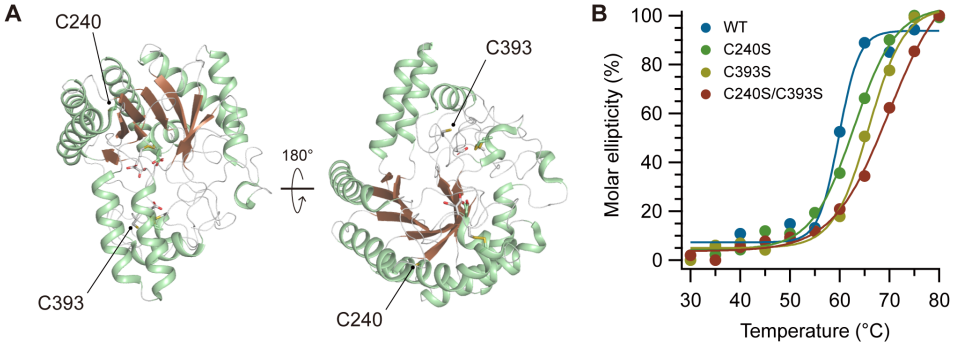

Fig. 4. (A) Distribution of secondary structure in *Pc*Cel6A. The helix, sheet, and loop regions in *Pc*-Cel6A apo structure (PDB ID 5XCY) [17] are colored green, brown, and light gray, respectively. The side chain of acid catalyst D216, candidate base catalysts D170 and D394, and Cys residues are shown as sticks in the same way as in Fig. 1. (B) Molar ellipticity at 214 nm of *Pc*Cel6A described to be the percentage with the minimum value as 0 % and the maximum value as 100 %.

Each sample comprised 0.8 μM *Pc*Cel6A in 2 mM sodium acetate (pH 5.0), 0.2 mM Tris-HCl (pH 8), and 0.2 mM NaCl. The solution without enzyme was used as a baseline.

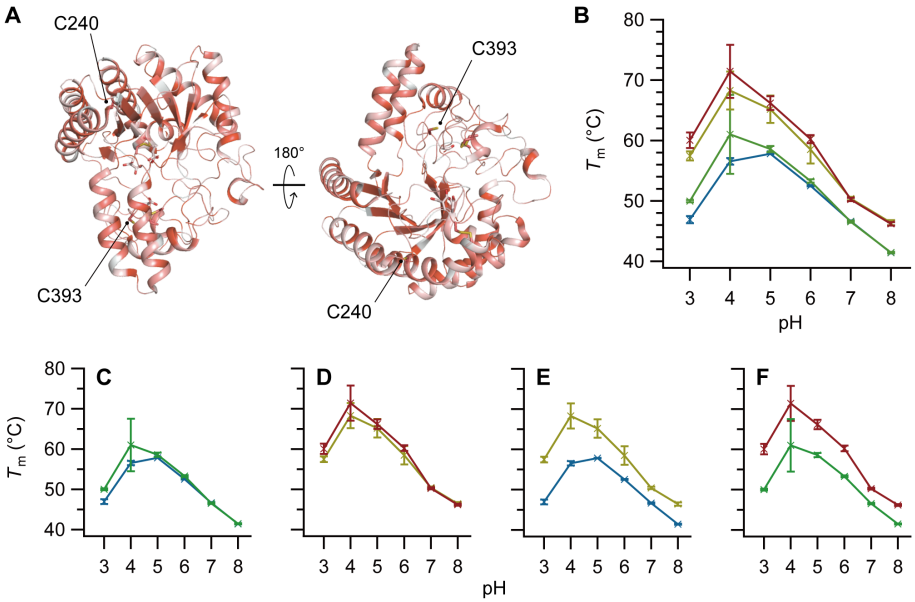

Fig. 5. (A) Distribution of hydrophobic regions in *Pc*Cel6A. Higher hydrophobicity in *Pc*Cel6A apo structure (PDB ID 5XCY) [17] is displayed in darker red. The side chain of acid catalyst D216, candidate base catalysts D170 and D394, and Cys residues are shown as sticks in the same way as in Fig. 1. (B–F) Melting temperature (T_m) in thermal shift assay of *Pc*Cel6A WT (blue), C240S (green), C393S (yellow), and C240S/C393S (red).

Each sample comprised 2 μg of protein, 50 mM buffer (pH 3, 6, 7, or 8 sodium phosphate and pH 4 or 5 sodium acetate), and 5x SYPRO™ Orange in 20 μL. $N = 4$. Error bars represent ±1 standard deviation.

[17]. In contrast, the distance from C393 to the closest Cys forming a disulfide bond, C361, was about 6 Å. Therefore, as suggested in the previous study of GH6 CBH [14], thiol-disulfide exchange might be involved in the thermal denaturation. This occurs when the thiolate anion of free Cys attacks the sulfur atom of a disulfide bond [36], and is thought to be involved in the thermal denaturation of enzymes [37]. Thus, C393 may undergo thiol-disulfide exchange with C361–C408 more readily than C240, and this could explain why substitution of C393 raised the T_m value more than substitution of C240.

A difference of the secondary structure in which free Cys is present might also influence the thermal denaturation behavior. C240 is located on the α-helix, whose main chain regularly forms hydrogen bonds, while C393 is on the long C-terminal loop consisting of 36 amino acids. Previous studies suggest that a long loop negatively impacts on thermal denaturation, because thermophiles possess a shorter loop [38] or loop deletion [39] compared with mesophiles. Therefore, C393 substitution within thermally unstable secondary structure might prevent intra/intermolecular thiol-disulfide exchange or the creation of a disulfide bond.

CONCLUSION

In this study, we investigated the characteristics of a thermotolerant double mutant C240S/C393S, which was previously created by substituting two free Cys residues in *Pc*Cel6A, based on a study of chimeric GH6 CBH in Arnold's lab. We focused on the activity at different temperatures and the change of folding with increasing temperature. C240S/C393S produced more cellobiose than the wild-type enzyme from both crystalline and amorphous cellulose at a high temperature, suggesting that substitutions of the free Cys residues make the catalytic domain more thermotolerant. While the activity of the catalytic domain at high temperature was decreased by replacing C240 with Ser, possibly due to steric effects, it was increased by substituting C393 with Ser. Substitution of each free Cys decreased thermal denaturation, though C393 substitution contributed more to the increase of thermal resistance than C240 substitution, possibly reflecting different interactions with adjacent residues. This will be discussed in detail in the accompanying paper (part II), based on X-ray crystal structure determination of each mutant.

CONFLICTS OF INTERESTS

The authors declare that they have no competing interests.

ACKNOWLEDGMENTS

We are grateful to Dr. Shinya Fushinobu at the University of Tokyo and Dr. Takatoshi Arakawa at the Tokyo University of Science for supporting the measurement of circular dichroism. SY is grateful for financial support from the UTokyo Sustainable Agriculture Education Program during a master's course. This study received financial support from Grants-in-Aid for Scientific Research (A) from the Japan Society for the Promotion of Science (JSPS) (No. 23H00341 to KI), the Sasakawa Scientific Research Grant from The Japan Science Society (No. 2021-4060 to SY), and a Grant-in-Aid for JSPS Fellows (No. 22J12651 to SY).

REFERENCES

[1] Lombard V, Golaconda Ramulu H, Drula E, Coutinho PM, Henrissat B. The carbohydrate-active enzymes database (CAZy) in 2013. Nucleic Acids Res. 2014; 42: 490−5.

[2] Abuja PM, Pilz I, Claessens M, Tomme P. Domain structure of cellobiohydrolase II as studied by small angle X-ray scattering: close resemblance to cellobiohydrolase I. Biochem Biophys Res Commun. 1988; 156: 180−5.

[3] Abuja PM, Schmuck M, Pilz I, Tomme P, Claeyssens M, Esterbauer H. Structural and functional domains of cellobiohydrolase I from *Trichoderma reesei*. Eur Biophys J. 1988; 15: 339−42.

[4] Medve J, Ståhlberg J, Tjerneld F. Adsorption and synergism of cellobiohydrolase I and II of *Trichoderma reesei* during hydrolysis of microcrystalline cellulose. Biotechnol Bioeng. 1994; 44: 1064−73.

[5] Igarashi K, Uchihashi T, Koivula A, Wada M, Kimura S, Okamoto T, et al. Traffic jams reduce hydrolytic efficiency of cellulase on cellulose surface. Science. 2011; 333: 1279−82.

[6] Badino SF, Christensen SJ, Kari J, Windahl MS, Hvidt S, Borch K. et al. Exo-exo synergy between Cel6A and Cel7A from *Hypocrea jecorina*: Role of carbohydrate binding module and the endo-lytic character of the enzymes. Biotechnol Bioeng. 2017; 114: 1639−47.

[7] Boisset C, Fraschini C, Schülein M, Henrissat B, Chanzy H. Imaging the enzymatic digestion of bacterial cellulose ribbons reveals the endo character of the cellobiohydrolase Cel6A from *Humicola insolens* and its mode of synergy with cellobiohydrolase Cel7A. Appl Environ Microbiol. 2000; 66: 1444−52.

[8] Voutilainen SP, Puranen T, Siika-Aho M, Lappalainen A, Alapuranen M, Kallio J, et al. Cloning, expression, and characterization of novel thermostable family 7 cellobiohydrolases. Biotechnol Bioeng. 2008; 101: 515−28.

[9] Wang XJ, Peng YJ, Zhang LQ, Li AN, Li DC. Directed evolution and structural prediction of cellobiohydrolase II from the thermophilic fungus *Chaetomium thermophilum*. Appl Microbiol Biotechnol. 2012; 95: 1469−78.

[10] Wu I, Arnold FH. Engineered thermostable fungal Cel6A and Cel7A cellobiohydrolases hydrolyze cellulose efficiently at elevated temperatures. Biotechnol Bioeng. 2013; 110: 1874−83.

[11] Heinzelman P, Snow CD, Wu I, Nguyen C, Villalobos A, Govindarajan S, et al. A family of thermostable fungal cellulases created by structure-guided recombination. Proc Natl Acad Sci USA. 2009; 106: 5610−5.

[12] Ito Y, Ikeuchi A, Imamura C. Advanced evolutionary molecular engineering to produce thermostable cellulase by using a small but efficient library. Protein Eng Des Sel. 2013; 26: 73−9.

[13] Heinzelman P, Snow CD, Smith MA, Yu X, Kannan A, Boulware K. et al. SCHEMA recombination of a fungal cellulase uncovers a single mutation that contributes markedly to stability. J Biol Chem. 2009; 284: 26229−33.

[14] Wu I, Heel T, Arnold FH. Role of cysteine residues in thermal inactivation of fungal Cel6A cellobiohydrolases. BBA- Proteins Proteom. 2013; 1834: 1539−44.

[15] Yamaguchi S, Sunagawa N, Tachioka M, Igarashi K, Samejima M. Thermostable mutants of glycoside hydrolase family 6 cellobiohydrolase from the basidiomycete *Phanerochaete chrysosporium*. J Appl Glycosci. 2020; 67: 79−86.

[16] Igarashi K, Maruyama M, Nakamura A, Ishida T, Wada M, Samejima M. Degradation of crystalline celluloses by *Phanerochaete chrysosporium* cellobiohydrolase II (Cel6A) heterologously expressed in methylotrophic yeast *Pichia pastoris*. J Appl Glycosci. 2012; 59: 105−10.

[17] Tachioka M, Nakamura A, Ishida T, Igarashi K, Samejima M. Crystal structure of a family 6 cellobiohydrolase from the basidiomycete *Phanerochaete chrysosporium*. Acta Crystallogr Sect F Struct Biol Commun. 2017; 73: 398−403.

[18] Nakamura A, Watanabe H, Ishida T, Uchihashi T, Wada M, Ando T, et al. Trade-off between processivity and hydrolytic velocity of cellobiohydrolases at the surface of crystalline cellulose. J Am Chem Soc. 2014; 136: 4584−92.

[19] Wada M, Chanzy H, Nishiyama Y, Langan P. Cellulose IIII crystal structure and hydrogen bonding by synchrotron X-ray and neutron fiber diffraction. Macromolecules. 2004; 37: 8548−55.

[20] Tachioka M, Sugimoto N, Nakamura A, Sunagawa N, Ishida T, Uchiyama T, et al. Development of simple random mutagenesis protocol for the protein expression system in *Pichia pastoris*. Biotechnol Biofuels. 2016; 9: 1−10.

[21] Eisenberg D, Schwarz E, Komaromy M, Wall R. Analysis of membrane and surface protein sequences with the hydrophobic moment plot. J Mol Biol. 1984; 179: 125−42.

[22] Brahms S, Brahms J, Spach G, Brack A. Identification of β,β-turns and unordered conformations in polypeptide chains by vacuum ultraviolet circular dichroism. Proc Natl Acad Sci USA. 1977; 74: 3208−12.

[23] Kabsch W, Sander C. Dictionary of protein secondary structure: Pattern recognition of hydrogen-bonded and geometrical features. Biopolymers. 1983; 22: 2577−637.

[24] Micsonai A, Wien F, Kernya L, Lee YH, Goto Y, Réfrégiers M, et al. Accurate secondary structure prediction and fold recognition for circular dichroism spectroscopy. Proc Natl Acad Sci USA. 2015; 112: E3095−103.

[25] Micsonai A, Wien F, Bulyáki É, Kun J, Moussong É, Lee YH, et al. BeStSel: A web server for accurate protein secondary structure prediction and fold recognition from the circular dichroism spectra. Nucleic Acids Res. 2018; 46: W315−22.

[26] Sreerama N, Woody RW. A self-consistent method for the analysis of protein secondary structure from circular dichroism. Anal Biochem. 1993; 209: 32−44.

[27] Sreerama N, Venyaminov SY, Woody RW. Estimation of the number of α-helical and β-strand segments in proteins using circular dichroism spectroscopy. Protein Sci. 1969; 8: 370−80.

[28] Rouvinen J, Bergfors T, Teeri T, Knowles JK, Jones TA. Three-dimensional structure of cellobiohydrolase II from *Trichoderma reesei*. Science. 1990; 249: 380−6.

[29] Spezio M, Wilson DB, Karplus PA. Crystal structure of the catalytic domain of a thermophilic endocellulase. Biochemistry. 1993; 32: 9906−16.

[30] Pantoliano MW, Petrella EC, Kwasnoski JD, Lobanov VS, Myslik J, Graf E, et al. High-density miniaturized thermal shift assays as a general strategy for drug discovery. J Biomol Screen. 2001; 6: 429−40.

[31] Stigter D, Alonso DOV, Dill KA. Protein stability: Electrostatics and compact denatured states. Proc Natl Acad Sci USA. 1991; 88: 4176−80.

[32] Volkin DB, Klibanov AM. Thermal destruction processes in proteins involving cystine residues. J Biol Chem. 1987; 262: 2945−50.
[33] Voorter CEM, De Haard-Hoekman WA, Van Den Oetelaar PJM, Bloemendal H, De Jong WW. Spontaneous peptide bond cleavage in aging α-crystallin through a succinimide intermediate. J Biol Chem. 1988; 263: 19020−3.
[34] Ahern TJ, Klibanov AM. The mechanism of irreversible enzyme inactivation at 100 °C. Science. 1985; 228: 1280−4.
[35] Wohlfahrt G, Pellikka T, Boer H, Teeri TT, Koivula A. Probing pH-dependent functional elements in proteins: Modification of carboxylic acid pairs in *Trichoderma reesei* cellobiohydrolase Cel6A. Biochemistry. 2003; 42: 10095−103.
[36] Gilbert HF. Thiol-disulfide exchange equilibria and disulfide bond stability. Methods Enzymol. 1995; 251: 8−28.
[37] Zale SE, Klibanov AM. Why does ribonuclease irreversibly inactivate at high temperatures. Biochemistry. 1986; 25: 5432−44.
[38] Russell RJM, Ferguson JMC, Hough DW, Danson MJ, Taylor GL. The crystal structure of citrate synthase from the hyperthermophilic archaeon *Pyrococcus furiosus* at 1.9 Å resolution. Biochemistry. 1997; 36: 9983−94.
[39] Thompson MJ, Eisenberg D. Transproteomic evidence of a loop-deletion mechanism for enhancing protein thermostability. J Mol Biol. 1999; 290: 595−604.
[40] Kelley LA, Mezulis S, Yates CAM, Wass MAN, Sternberg MJE. The Phyre2 web portal protein modeling, prediction, and analysis. Nat Protoc. 2016; 10: 845−58.
[41] Payne CM, Bomble YJ, Taylor CB, McCabe C, Himmel ME, Crowley MF. Multiple functions of aromatic-carbohydrate interactions in a processive cellulase examined with molecular simulation. J Biol Chem. 2011; 286: 41028−35.